The role of surface reactions on the active and selective catalyst design for bioethanol steam reforming

M. Benito [a,b,*], R. Padilla [a], A. Serrano-Lotina [a], L. Rodríguez [a], J.J. Brey [c], L. Daza [a]

[a] Instituto de Catálisis y Petroleoquímica (CSIC), C/Marie Curie 2, Campus Cantoblanco, 28049 Madrid, Spain
[b] Ciemat, Av. Complutense 22, 28040 Madrid, Spain
[c] Hynergreen Technologies, Av. Buhaira 2, 41018 Sevilla, Spain

ARTICLE INFO

ABSTRACT

In order to study the role of surface reactions involved in bioethanol steam reforming mechanism, a very active and selective catalyst for hydrogen production was analysed. The highest activity was obtained at 700 °C, temperature at which the catalyst achieved an ethanol conversion of 100% and a selectivity to hydrogen close to 70%. It also exhibited a very high hydrogen production efficiency, higher than 4.5 mol H_2 per mol of EtOH fed. The catalyst was operated at a steam to carbon ratio (S/C) of 4.8, at 700 °C and atmospheric pressure. No by-products, such as ethylene or acetaldehyde were observed. In order to consider a further application in an ethanol processor, a long-term stability test was performed under the conditions previously reported. After 750 h, the catalyst still exhibited a high stability and selectivity to hydrogen production. Based on the intermediate products detected by temperature programmed desorption and reaction (TPD and TPR) experiments, a reaction pathway was proposed. Firstly, the adsorbed ethanol is dehydrogenated to acetaldehyde producing hydrogen. Secondly, the adsorbed acetaldehyde is transformed into acetone via acetic acid formation. Finally, acetone is reformed to produce hydrogen and carbon dioxide, which were the final reaction products. The promotion of such reaction sequence is the key to develop an active, selective and stable catalyst, which is the technical barrier for hydrogen production by ethanol reforming.

© 2009 Elsevier B.V. All rights reserved.

1. Introduction

Hydrogen is a clean and free carbon energy vector that can be used directly in thermal combustion engines or converted into electrical energy using fuel cells. Nowadays, most of hydrogen is obtained from fossil fuels by reforming processes.

Natural gas or methane represents the main option for hydrogen production from fossil fuels, whose energetic efficiency is three times higher than water electrolysis when the electricity used to support the endothermic reforming process is obtained from fossil fuels [1,2]. At the moment, there are many papers published in literature concerning gasoline, diesel or jet propulsion fuel reforming, specially oriented to on-board applications [3]. From this standpoint, reforming of conventional fuels may represent an option to facilitate the transition to hydrogen economy by using the actual logistic infrastructure. Given that hydrogen is obtained from fossil fuels, what does not avoid the emission of greenhouse gases, is

not possible to consider it as 'green hydrogen'. In order to avoid such emissions, the use of biomass or bio-fuels for hydrogen production may represent a very good option to partially satisfy the demand of energy. Using bioethanol for hydrogen production could be an attractive alternative to minimize negative environmental concerns and to decentralise the actual fuel market, in which few countries or geographical areas control Global Development and Economy [4,5]. Ethanol advantages as a fuel come from the fact that it can be used in internal combustion engines or transformed into hydrogen for fuel cells operation, using the actual logistic system.

On one hand, growing crops for bio-fuels is being criticized because of its direct competition for land and food production. On the other hand, the European Commission determined in 2006, that the influence of bio-fuels on corn prices was marginal and represented a 3–6% of corn price [6]. Muller et al. [7] reported that even with an expanding world population, globally there is still enough land and water to grow a substantial amount of biomass for both, food and bio-energy production.

Taking into consideration scientific aspects, many papers have been published in recent years for hydrogen production from ethanol reforming. Initial articles based on thermodynamic studies, which determined the experimental conditions to maximize

* Corresponding autor at: Instituto de Catálisis y Petroleoquímica (CSIC), C/Marie Curie 2, Campus Cantoblanco, 28049 Madrid, Spain. Tel.: +34 91 5854793; fax: +34 91 5854760.
E-mail address: mjbenito@icp.csic.es (M. Benito).

hydrogen production, are remarkable [8–10]. Regarding to catalysts studies, preliminary works used precious metal such as Pt or Rh as active phase. In such cases, considering an industrial application, the use of noble metals does not represent a realistic option in conventional applications. Its application could be reduced just to special technological markets where cost is not the priority, i.e. military applications.

Coke deposition was identified as the main cause for catalyst deactivation in nickel-based catalysts, being identified coke depletion as the goal for catalyst development [11]. Carbon can be formed by Boudouard's reaction, methane decomposition and ethylene, formed by ethanol dehydration, polymerization. Some authors [12,13] tried to overcome catalyst deactivation by the addition of an alkaline promoter to nickel catalysts supported on alumina. They diminished the deactivation rate but did not solve the problem. Other authors investigated other catalytic supports which presented basic properties, i.e. MgO as another *via* to avoid coke deposition [14]. Vargas et al. [15] developed catalysts supported on oxides with a high oxygen mobility based in Ce–Zr–Co fluorite structure. Other studies were focused on studies of the influence of the active phase. Llorca et al. [16] studied cobalt-based catalyst as an alternative to nickel activity and stability.

Most of papers postulated a mechanism that promotes dehydrogenation reaction *vs.* dehydration as the key to optimize hydrogen production and catalyst stability. From this standpoint, Noronha and coworkers [17] proposed different pathways. After the adsorption of ethanol on catalyst surface as ethoxy species, it can be decomposed to CO, CH_4 and H_2 or to acetaldehyde and acetyl species, following the dehydrogenation *via*. The dehydrogenated species may undergo oxidation to acetate species. Water not only promotes oxidation processes but also decomposition of acetate species producing CH_4, CO and carbonate.

Fatsikostas and Verykios [18] determined the reaction network of ethanol steam reforming over Ni-based catalyst employing transient and steady-state techniques. They suggested that catalyst support plays an important role to promote dehydrogenation *vs.* dehydration reactions. On alumina Ni supported catalysts, ethanol strongly interacts with the support, promoting ethanol dehydration at low temperatures while on lanthana supports, ethanol interacts less strongly, what promotes both, ethanol dehydrogenation and dehydration. Cracking reactions were also detected at intermediate temperatures. In addition to the reactions mentioned above, reforming, water-gas-shift and methanation reactions contributed significantly to the final product distribution.

In a previous paper [19], a tentative pathway for ethanol steam reforming based on by-products, detected when gas hourly space velocity (GHSV) was increased at high temperature, was proposed. An increase of acetaldehyde and a minor increase in ethylene concentration in the product distribution were detected. These results allowed us to establish that favouring ethanol dehydrogenation to acetaldehyde against dehydration to ethylene can be the key to obtain an active and stable catalyst. The use of temperature programmed desorption and reaction experiments of ethanol, acetaldehyde and acetone can determine the role of surface reactions involved in ethanol steam reforming reaction. For that purpose, a catalyst [20] based on cobalt as active phase and supported on zirconia promoted by lanthana, was studied. It demonstrated a very high activity, selectivity to hydrogen production and a great stability in ethanol steam reforming.

The aim of this work was to determine intermediate reaction species in ethanol steam reforming in order to propose the surface reactions involved in reaction mechanism that conduce to such activity, selectivity to hydrogen and stability, probably the most important feature for ethanol steam reforming reaction.

2. Experimental

2.1. Catalyst preparation

The catalyst used to perform this study was based on cobalt as the active phase supported on zirconia promoted by lanthana. It was prepared by impregnation in dissolution method, dried overnight at 110 °C and calcined at 800 °C. The details of catalyst preparation were patented [20].

2.2. Temperature programmed desorption (TPD) and reaction (TPR) experiments

TPD and TPR experiments were performed with a Mettler-Toledo TGA/SDTA 851^e thermo-balance, being the experimental data recorded with the software STAR 8.10. Thermo-balance was coupled to a mass spectrometer detector Pfeiffer Thermostar. Catalyst samples (100 mg approximately) were submitted to an Argon flow (50 ml min^{-1}) which was saturated separately with ethanol, acetone and acetaldehyde. Temperature programmed reaction experiments (TPR) with steam/carbon ratio (S/C) of 4.8 for ethanol and ethanol and acetaldehyde aqueous solutions and S/C = 3.2 for acetone aqueous solution were performed.

After 20 min in contact with the Ar saturated stream at 25 °C, the catalytic sample was heated to 900 °C at 15 °C min^{-1} using an Ar stream (50 ml min^{-1}). The evolution of m/z 2, 15, 18, 26, 28, 29, 30, 44, 45, 46, 58, 74, that correspond to H_2, CH_4, H_2O, ethylene, CO, acetaldehyde, ethane, CO_2, ethanol, acetone and diethyl-ether, respectively, were recorded.

2.3. Reaction experiments

Reaction experiments were performed in order to study the influence of temperature on ethanol conversion, H_2/ethanol ratio and the product distribution, respectively. Reaction tests started at 700 °C and decreased to 500 °C in steps of 25 °C, maintaining these steps for 3 h. Another stability test at 700 °C, S/C = 4.8 and GHSV = 61,000 h^{-1} was performed for 700 h.

Reaction tests were performed introducing bioethanol and water, without a gas carrier, in order to simulate the conditions expected in a real fuel processor.

The parameters used to study the catalytic activity were ethanol conversion, denoted as X_{EtOH}, and product distribution denoted as Y_i. These parameters were calculated by the following Eqs. (i) and (ii):

$$X_{EtOH} = \left(\frac{\text{moles } EtOH_{in} - \text{moles } EtOH_{out}}{\text{moles } EtOH_{in}} \right) \times 100 \tag{i}$$

$$Y_i = \left(\frac{\text{moles } P_i}{\sum \text{moles } P_i} \right) \times 100 \tag{ii}$$

P_i: reaction products.

Gas hourly space velocity was calculated by the following mathematical Eq. (iii):

$$GHSV = \frac{Q_{reactants}}{V_{catalytic bed}} \tag{iii}$$

The reaction apparatus is equipped with mass flow controllers to adjust the pre-treatment gas flow and an isocratic pump to control the liquid feed with a very good accuracy. A SCADA software for data acquisition and control for the different reaction parameters was used. A catalyst sample (100 mg) was introduced in a fixed bed quartz tubular reactor with an o.d. of 9.52 mm.

Chromatography was the analytical technique used to evaluate the composition of reaction products. In order to separate permanent gases (H_2, CO and CH_4), a 5 Å molecular sieve column was
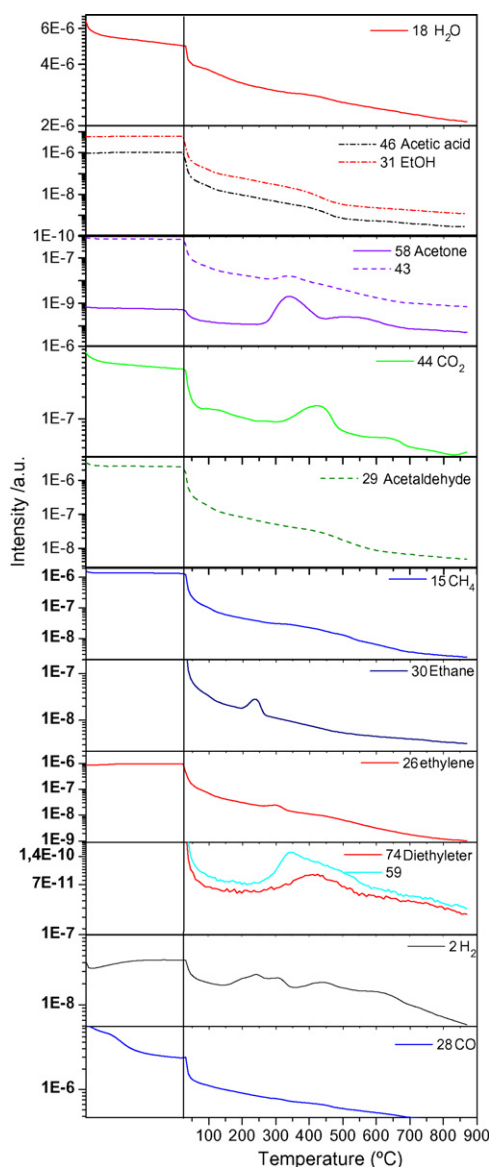
Fig. 1. TPD experiment performed with ethanol.

drogenation to obtain acetaldehyde (reactions (1) and (2)) [21,22]:

$$CH_3CH_2OH \rightleftarrows CH_3CH_2OH_{ads} \quad (1)$$

$$CH_3CH_2OH \rightleftarrows CH_3CHO_{ads} + H_2 \quad (2)$$

After 200 °C, ethane and H_2 are detected simultaneously. H_2 can come from acetaldehyde reforming (reaction (3)) with H_2O previously adsorbed at room temperature. By acetaldehyde thermal decomposition (reaction (4)) or decarbonilation (reaction (5)), methyl groups could be obtained. Reactions (5) and (6) can also explain CO traces. The broad peak ascribed to methane desorption can be explain by reaction (7). H_2 and CO_2 production can be compatible with water-gas-shift reaction (reaction (8)), thermodynamically favoured at low temperatures. Ethane can be formed by coupling reaction of two methyl groups adsorbed (reaction (9)) or by free methyl radical reaction formed by acetaldehyde thermal decomposition (reaction (4)) [23].

$$CH_3CHO_{ads} + H_2O \rightleftarrows 2CO + 3H_2 \quad (3)$$

$$CH_3CHO_{ads} \rightleftarrows CH_3{}^* + CHO^* \quad (4)$$

$$CH_3CHO_{ads} \rightleftarrows CO_{ads} + CH_{3\,ads} + H_{ads} \quad (5)$$

$$CO_{ads} \rightleftarrows CO \quad (6)$$

$$CH_{3\,ads} + H_{ads} \rightleftarrows CH_4 \quad (7)$$

$$CO_{ads} + H_2O_{ads} \rightleftarrows H_2 + CO_2 \quad (8)$$

$$CH_{3\,ads} + CH_{3\,ads} \rightleftarrows C_2H_6 \quad (9)$$

Between 250 and 450 °C, acetone, diethyl-ether and ethylene traces were detected as well as H_2. Acetone could be obtained by reaction of two ethanol molecules adsorbed (reaction (10)) [24].

$$2CH_3CH_2OH_{ads} \rightleftarrows CH_3COCH_3 + 3H_2 + CO \quad (10)$$
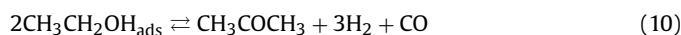
Idriss et al. [25] reported that acetone was produced by acetaldehyde reaction with methyl groups adsorbed (reaction (11)), and that diethyl-ether can be obtained by the reaction between acetaldehyde molecules adsorbed (reaction (12)). However, Mariño et al. [26] suggested that diethyl-ether was formed by reaction of two ethanol molecules accomplished of water formation. Ethylene can be formed by ethanol dehydration (reaction (13)).

$$CH_3CHO_{ads} + CH_{3\,ads} \rightleftarrows CH_3COCH_3 \quad (11)$$

$$2CH_3CHO_{ads} \rightleftarrows CH_3CH_2OCH_2CH_3 + H_2 \quad (12)$$

$$CH_3CH_2OH \rightleftarrows C_2H_4 \quad (13)$$

At 350 °C, a decrease in the peak ascribed to acetone desorption was observed. This fact took place simultaneously with a m/z signal increase of CO_2 and H_2 that achieved a maximum at 430 °C which could be explained by acetone reforming with the residual water present on the catalyst surface that was adsorbed at room temperature (reaction (14)). This fact can be observed again at 600 °C.

$$CH_3COCH_3 + H_2O \rightleftarrows 3CO_2 + 8H_2O \quad (14)$$

In the temperature range studied (250–450 °C), a wide desorption peak ascribed to CH_4 was detected. It could be obtained by decarboxilation of acetate species at high temperature [27]. Between 495 and 655 °C, H_2 and CO_2 desorption was detected, while acetone and diethyl-ether decreased. This fact can be explained by the reforming reaction contribution (reaction (14)).

used, while hydrocarbons and CO_2 were separated in a Porapak Q column. The chromatograph (Agilent 6890 N) is equipped with TCD and FID detectors connected in line. As possible steam reforming by-products can appear, a mass spectrometer (Agilent 5973) connected to a GC chromatograph was used.
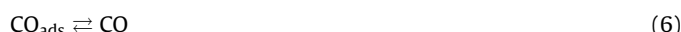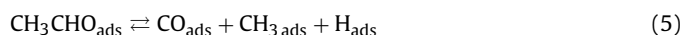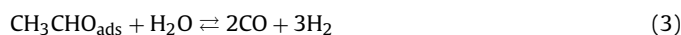
3. Results and discussion

3.1. Ethanol TPD

In order to identify intermediate products formed in the reaction, a TPD test using Ar saturated stream in ethanol at 25 °C was performed. Fig. 1 compiles the evolution of the different m/z that correspond to main and secondary reaction products detected as a consequence of the surface reaction on the catalyst studied.

After 20 min in isothermal conditions at 25 °C the heating ramp started. At 100 °C small peaks ascribed to the desorption of H_2O and CO_2 previously adsorbed on the catalyst sample were detected. At 160 °C, H_2 desorption was observed as the result of ethanol dehy-
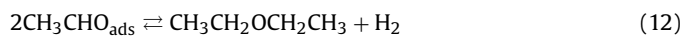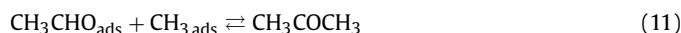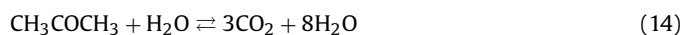
3.2. Ethanol–water TPR

Having analyzed the reaction products obtained by the surface reaction of the adsorbed ethanol, the influence of water in the reforming reaction became an interesting study to perform. Fig. 2 compiles the evolution of different m/z signal ascribed to reaction
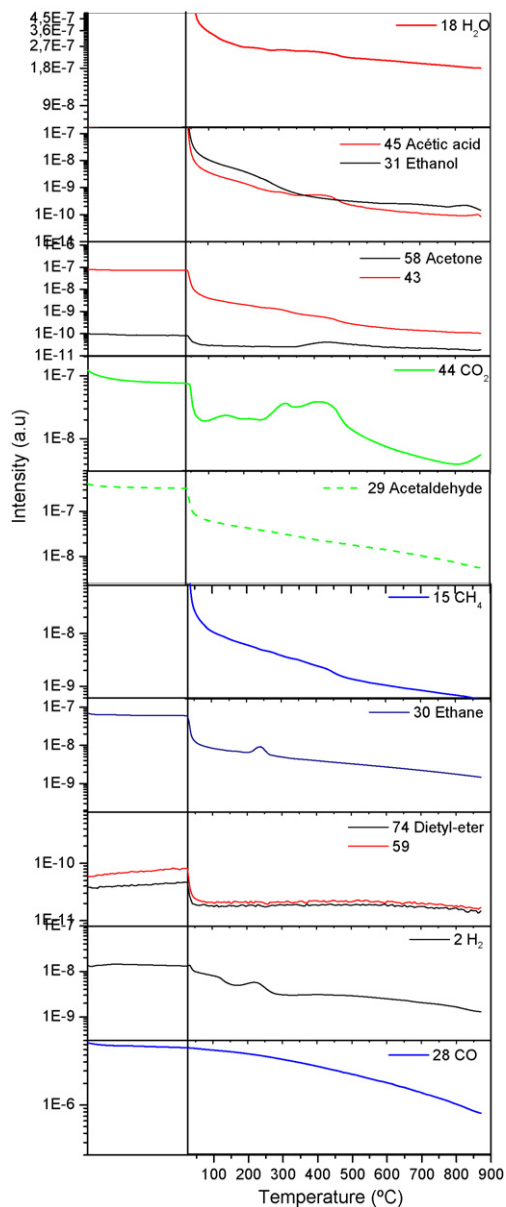
Fig. 2. TPR experiment performed with a dissolution ethanol–water.

and secondary products and by-products in ethanol steam reforming reaction when Ar stream was saturated in an ethanol/water dissolution with a S/C = 4.8 at 25 °C for 20 min.

The adsorption of the solution of water and ethanol produces changes in the distribution of the observed desorption products. The simultaneous desorption of H_2 and CO_2 at low temperature (135 °C) which corresponds to final products of a reforming process, was detected.

While from 217 °C, a peak ascribed to hydrogen desorption was detected, there was no peak for carbon dioxide. This fact is noteworthy and can be explained by ethanol dehydrogenation reaction to acetaldehyde (reaction (2)).

Contrary to the previous test, a peak desorption ascribed to ethylene (298 °C) was not detected, leading us to think that water presence can inhibit the ethanol dehydration reaction.

From 304 °C, a new desorption peak ascribed to CO_2, previous to the acetone desorption (430 °C), can be observed, which can establish the temperature at which acetone is formed. In this experiment the desorption peak ascribed to acetone (430 °C) showed a much

smaller intensity which appears simultaneously with CO_2 desorption, what confirmed acetone reforming reaction (reaction (14)).

Therefore, as a consequence of intermediate products detected, we can assume that water presence inhibits the ethanol dehydration vs. the dehydrogenation to acetaldehyde, that once adsorbed on catalyst surface would evolve towards the acetone yield.

According to the reaction sequence proposed, and based on the TPR experiments, the catalyst partially inhibits the reactions responsible for the coke formation via ethylene, with the exception of the possible coke formed by Boudouard's reaction (thermodynamically possible).

3.3. Acetaldehyde–water TPR

Once identified that ethanol dehydrogenation produces acetaldehyde as previous step in the reforming process, it is necessary to deepen in the possible surface reactions that take place when acetaldehyde is adsorbed. For that purpose, a TPR test using an acetaldehyde aqueous solution was performed. Fig. 3 compiles the evolution of different m/z signals recorded in the TPR experiment. At low temperature (150 °C), a desorption peak ascribed to
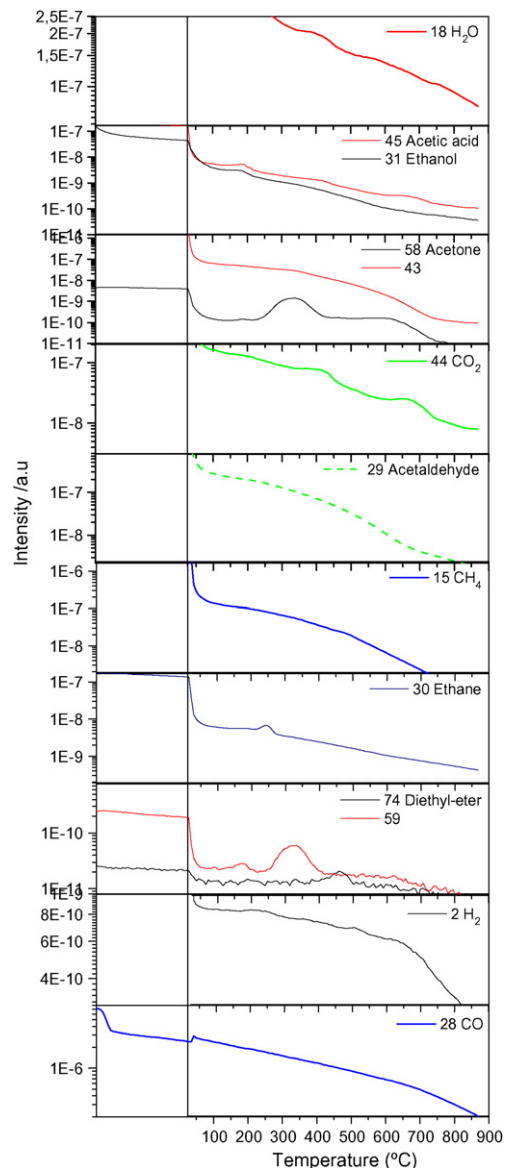

Fig. 3. TPR experiment performed with a dissolution acetaldehyde–water.

ethanol was detected. Ethanol produced apparently comes from acetaldehyde hydrogenation which indicates a reversible process [28]. Three desorption peaks ascribed to acetic acid desorption ($m/z = 45$) were detected at 183, 416 and 670 °C. Two broad peaks ascribed to acetone desorption were detected at 329 and 641 °C, which were shifted to higher temperature in relation with acetic acid desorption peaks. It is important to note that acetone formation from ethanol reforming is possible at low temperature due to ΔG becomes negative at 91 °C. Three important routes have been proposed to the transition from acetaldehyde to acetone:

Nakajima et al. [29,30] proposed a pathway which involves the acid acetic formation as the key intermediate and a further bimolecular arrangement leading to acetone and carbon dioxide as the most important compounds. Sreerama et al. [31] suggested aldol condensation of acetaldehyde while Idriss et al. [25] proposed a reaction between acetyl and methyl species. At the light of the results obtained in our study, acetone can be preferably obtained *via* acetic acid as opposed to the mechanism proposed by Zhang et al. [28] in which acetaldehyde is transformed into methane by the decomposition reaction. However, a low intensity broad desorption peak ascribed to methane desorption was detected. It is noteworthy the absence of the CO desorption peak, which indicates that water-gas-shift reaction was promoted.

3.4. Acetone–water TPR

A TPR with aqueous acetone dissolution was performed (Fig. 4). CO_2 was the only product detected in the temperature range studied. Traces of acetic acid ($m/z = 45$) at 424 and 644 °C indicated the reversibility of the process. Carbon dioxide desorption peaks at 174, 307, 426 and 672 °C indicated that acetone was chemisorbed on different catalytic sites with different strength. CO_2 peak sequence corresponded with a broad acetone desorption peak detected from room temperature up to 700 °C, which indicated that acetone is reformed to produce hydrogen and carbon dioxide as final reaction products.

3.5. Activity testing

Fig. 5 represents ethanol conversion and H_2/EtOH ratio evolution *vs.* temperature. It is remarkable that ethanol fed was totally converted at temperature higher than 550 °C. An increase in temperature leads to a H_2/EtOH ratio up to 5.9 at 675 °C, temperature at which thermodynamics predict the maximum value, due to the minimization of methane concentration [32]. It also produced an increase in CO concentration because water-gas-shift reaction is not promoted at high temperatures (Fig. 6). While carbon dioxide remains constant in the temperature range considered, methane decreases from 2.53 at 550 °C to 1.72 at 650 °C. This fact suggests that methane is reformed to produce carbon monoxide and hydrogen. A further increase on temperature produced a decrease of hydrogen concentration due to ethane formation. At low temperature (500 °C) the presence of acetone as an intermediate product (3.5%), was detected (Fig. 7). It was also determined by TPR–TPD experiments showed previously. This fact is minimized at temperature higher than 600 °C. The presence of ethylene, resulting from ethanol dehydration reaction, was negligible and decreased with temperature. The low acetaldehyde concentration <500 ppmV suggests a quick transformation into acetone at temperatures as low as 500 °C.

Trying to determine the activity, selectivity and stability of the catalyst studied, a long-term reaction test in catalytic activity conditions was submitted. Fig. 8 shows the evolution of the ethanol conversion and H_2/EtOH ratio *vs.* time. Ethanol conversion achieved 100% and was totally stable for approximately 800 h in reaction conditions. H_2/EtOH ratio shows a slow but continuous increase with
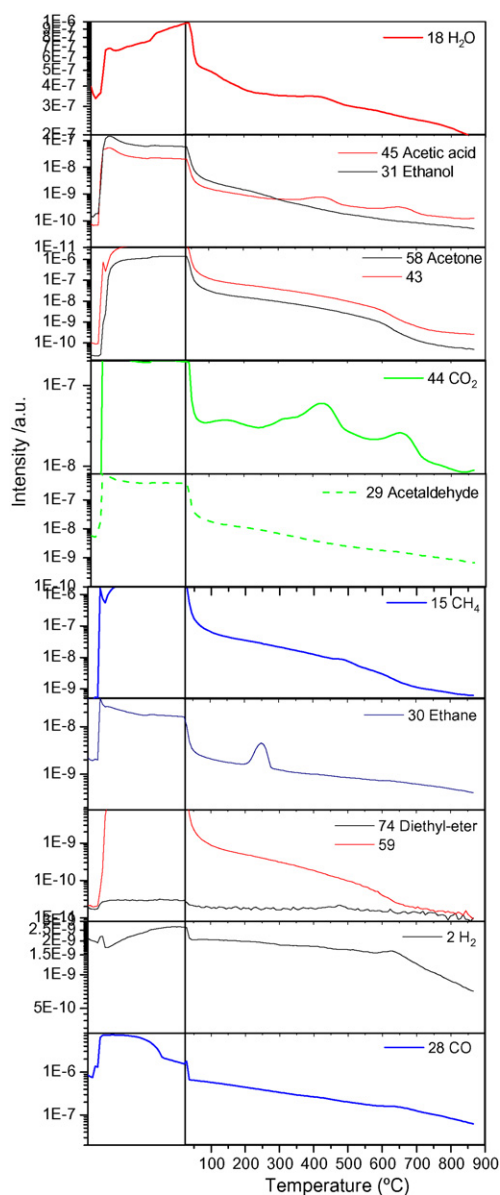

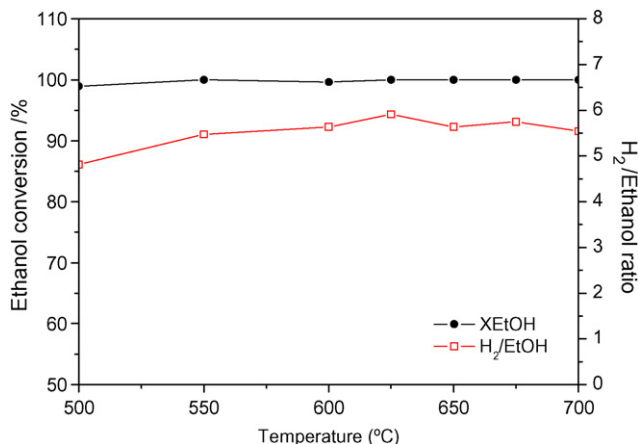**Fig. 4.** TPR experiment performed with a dissolution acetone–water.

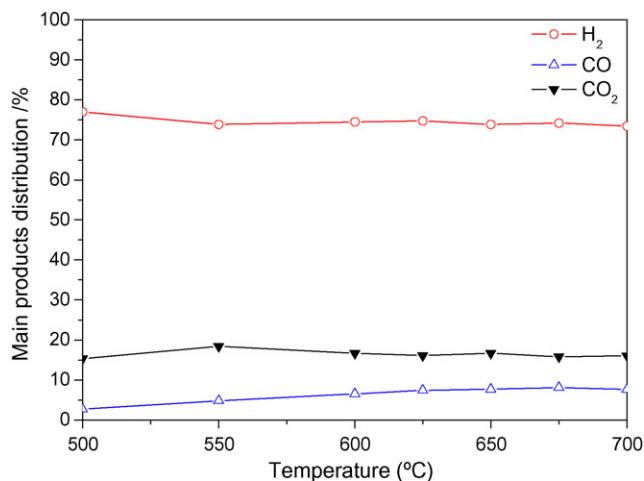**Fig. 5.** Temperature influence in ethanol conversion and H_2/EtOH ratio.

Fig. 6. Temperature influence in main products distribution.

Fig. 9. Products distribution in a long-term reaction test at 700 °C.

reaction time up to 4.5 mol of H_2 per mol of ethanol fed, which can suggest an activation of the catalyst.

This high efficiency is directly related to the reaction displacement towards the formation of final products as H_2 and CO_2. CO_2 concentration next to 20% as opposed to CO concentration (10%) confirms this fact (Fig. 9).
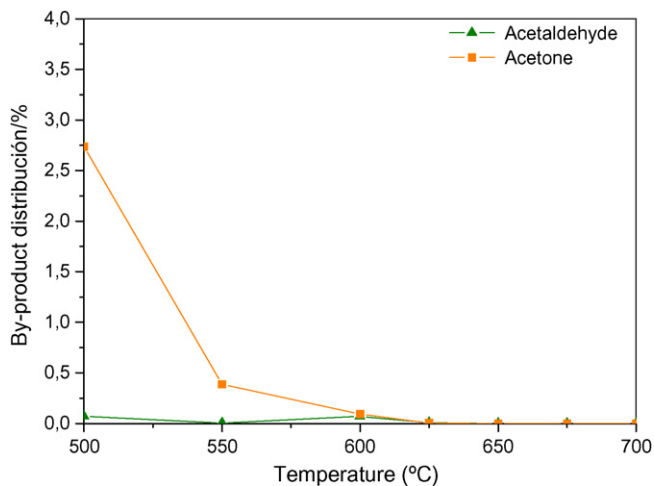

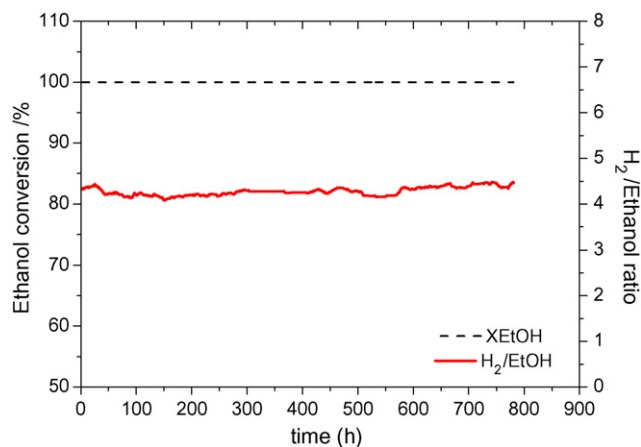**Fig. 7.** Temperature influence in by-products distribution.

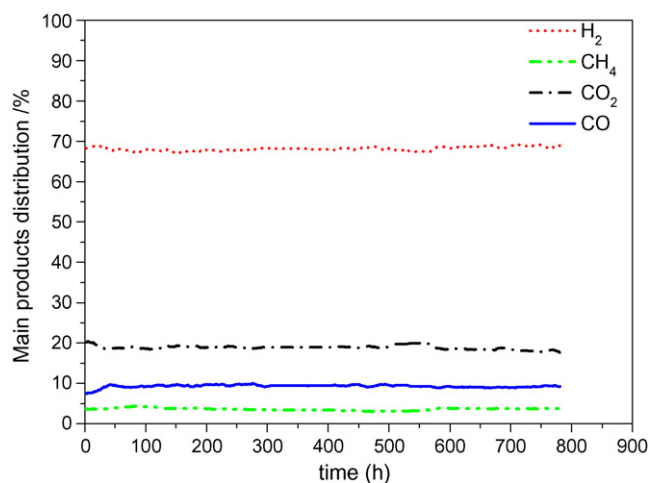**Fig. 8.** Ethanol conversion and H_2/EtOH ratio in a long-term reaction test at 700 °C.

It is well known that water-gas-shift reaction takes an important role in the product distribution. WGS reaction is thermodynamically favoured at low temperatures, however, the experimental results show a high displacement of the reaction at high temperature, what means a high hydrogen concentration (70% approx.) and low methane concentration (3.8% approximately). This 800 h stability test is remarkable due to the few papers that perform long-term stability tests. Verykios and coworkers [33] reported long-term stability results (45 h) obtained with a nickel supported on lanthana catalyst. Their catalyst showed high activity and selectivity to hydrogen production, at 600 °C and ethanol:water ratio 1:3. Using a catalyst consisting on ruthenium supported on alumina [34] a long-term stability test was performed at 700 °C and H_2O/EtOH ratio 2:1, which showed a low deactivation rate after 100 h (15% of ethanol conversion loss). Shen and coworkers [28] reported long-term stability results obtained with a catalyst based on Ir supported on CeO_2. This catalyst operated stable for more than 800 h, while other catalysts based on transition metal oxides (Ni, Co) supported on CeO_2 showed a significant deactivation even for 25 h.

4. Conclusions

Temperature programmed desorption and reaction experiments allowed us to determine the involved intermediate species in the reaction mechanism for ethanol steam reforming in a catalyst based on cobalt supported on zirconia promoted by lanthana. The catalyst promotes ethanol dehydrogenation reaction to acetaldehyde. Acetaldehyde adsorbed on catalyst surface reacts *via* acetic acid for acetone production. Acetone reforming reaction could take place from 400 °C to produce H_2 and CO_2.

The studied catalyst showed a great activity and selectivity to hydrogen production in the conditions tested (700 °C, S/C = 4.8), without showing deactivation after 800 h in reaction conditions. Hydrogen efficiency production was 4.5 mol H_2 per mol of ethanol fed, at 700 °C and atmospheric pressure, which represents an efficiency around 82% *vs.* the equilibrium estimation.

The promotion of ethanol dehydrogenation to acetaldehyde, the acetone production from acetaldehyde and its reforming were the key steps in the reaction pathway that allow to develop an active, selective and stable catalyst, which is the technical barrier for hydrogen production by ethanol reforming.

The results obtained allow us to implement the studied catalyst in an ethanol processor for hydrogen production.

References

[1] P. Ferreira-Aparicio, M. Benito, J.L. Sanz, Catal. Rev. 47 (2005) 491–588.
[2] I. Dincer, Int. J. Hydrogen Energy 27 (2002) 265–285.
[3] S. Roychoudhury, M. Lyubovsky, D. Walsh, D. Chu, E. Kallio, J. Power Sources 160 (2006) 510–513.
[4] ENREL, US, Department of Energy, DOE/GO-10097-515, November 1997.
[5] J. Eaves, S. Eaves, Energy Policy 35 (2007) 5958–5963.
[6] European Commission, The impact of a minimum 10% obligation for biofuel use in the EU-27 in 2020 on agricultural markets, 2007.
[7] A. Müller, J. Schmidhuber, J. Hoogeveen, P. Steduto, Water Policy 10 (2008) 83–94.
[8] E.Y. García, M.A. Laborde, Int. J. Hydrogen Energy 16 (1991) 212–307.
[9] K. Vasudeva, N. Mitra, P. Umasankar, S.C. Dhingra, Int. J. Hydrogen Energy 21 (1996) 13–18.
[10] I. Fishtik, A. Alexander, R. Datta, D. Geane, Int. J. Hydrogen Energy 25 (2000) 31–45.
[11] A.L. Alberton, M.M.V.M. Souza, M. Schmal, Catal. Today 123 (2007) 257–264.
[12] F. Mariño, M. Boveri, G. Baronetti, Int. J. Hydrogen Energy 26 (2001) 665–668.
[13] A.J. Vizcaino, P. Arena, G. Baronetti, A. Carrero, J.A. Calles, M.A. Laborde, N. Amadeo, Int. J. Hydrogen Energy 26 (2008) 3489–3492.
[14] M.S. Batista, R.K.S. Santos, E.M. Assaf, J.M. Assaf, E.A. Ticianelli, J. Power Sources 124 (2003) 99–103.
[15] J.C. Vargas, S. Libs, A. Roger, A. Kiennemann, Catal. Today 107–108 (2005) 417–425.
[16] J. Llorca, N. Homs, J. Sales, P.R. Piscina, J. Catal. 209 (2002) 3016–3017.
[17] S.M. de Lima, I.O. da Cruz, G. Jacobs, B.H. Davis, L.V. Mattos, F.B. Noronha, J. Catal. 257 (2008) 356–368.
[18] A.N. Fatsikostas, X.E. Verykios, J. Catal. 225 (2004) 439–452.
[19] M. Benito, J.L. Sanz, R. Isabel, R. Padilla, R. Arjona, L. Daza, J. Power Sources 151 (2005) 11–17.
[20] M. Benito, J.L. Sanz, R. Isabel, L. Daza, Patent WO2006075035A1.
[21] M. Bowker, H. Houghton, K.C. Waugh, J. Chem. Soc. Faraday Trans. 1 (78) (1982) 2573.
[22] M. Bowker, R.W. Petts, K.C. Waugh, J. Catal. 99 (1986) 53.
[23] A. Kayode Coker, Modelling of Chemical Kinetics and Reactor Design, Gulf Publishing Company, Hoston, TX, 2001, ISBN 088415-481-5.
[24] B. Zhang, X. Tang, Y. Li, W. Cai, Y. Xu, W. Shen, Catal. Commun. 7 (2006) 367–372.
[25] H. Idriss, C. Diagne, J.P. Hindermann, A. Kiennemann, M.A. Barteau, J. Catal. 155 (1995) 219–237.
[26] F. Mariño, M. Boveri, G. Baronetti, M. Laborde, Int. J. Hydrogen Energy 26 (2001) 665–668.
[27] J. Bussi, S. Parodi, B. Irigaray, R. Kieffer, Appl. Catal. A: Gen. 172 (1998) 117–129.
[28] B. Zhang, W. Cai, Y. Li, Y. Xu, W. Shen, Int. J. Hydrogen Energy 33 (2008) 4377–4386.
[29] T. Nakajima, H. Nameta, S. Mishima, I. Matsuzake, K. Tanabe, J. Mater. Chem. 4 (6) (1994) 853–858.
[30] T. Nakajima, K. Tanabe, T. Yamaguchi, I. Matsuzake, S. Mishima, Appl. Catal. 52 (1989) 237–248.
[31] R. Sreerama, P. Patmaik, P. Sidheswaran, M. Jayamani, J. Catal. 109 (1988) 298–302.
[32] M. Benito, R. Padilla, J.L. Sanz, L. Daza, J. Power Sources 169 (2007) 123–130.
[33] A.N. Fatsikostas, D.I. Kondarides, X.E. Verykios, Catal. Today 75 (2002) 145–155.
[34] D.K. Liguras, D.I. Kondarides, X.E. Verykios, Appl. Catal. B: Environ. 43 (2003) 345–354.